

Article

Multitemporal Incidence of Landscape Fragmentation in a Protected Area of Central Andean Ecuador

Carlos Rosero ^{1,*}, Xosé Otero ², Cinthya Bravo ¹ and Catherine Frey ^{1,*}

¹ Grupo de Investigación y Desarrollo para el Ambiente y Cambio Climático, Facultad de Ciencias, Escuela Superior Politécnica de Chimborazo, Panamericana Sur Km 1 1/2, Riobamba 060155, Ecuador

² CRETUS, Departamento de Edafología e Química Agrícola, Universidade Santiago de Compostela, Campus Vida, 15782 Santiago de Compostela, Spain

* Correspondence: carlos.rosero@esPOCH.edu.ec (C.R.); catherine.frey@esPOCH.edu.ec (C.F); Tel.: +593-987-718036 (C.R.)

Abstract: Monitoring land cover changes in protected areas is crucial to control the conservation efficiency of biodiversity and natural ecosystem conditions, especially in Ecuador, one of the most megadiverse countries in the world. Therefore, the purpose of the present study has been to estimate spatiotemporal changes in the landscape and the level of fragmentation using remote sensing in Llanganates National Park (PNL), a protected area in central Andean Ecuador. To obtain land cover, satellite images were processed using the Maximum Likelihood Classification (MLC) algorithm. After statistical analysis, it was encountered that there is no significant difference in land cover change between the years 1991 to 2016 nor among the three watersheds, while the level of fragmentation in the PNL is low. Land cover changes in the study area are not evident, as it is a protected area where ecosystems are usually expected to maintain their initial conditions over time. Therefore, with these results it has been concluded that the biodiversity and landscape conservation processes in the PNL are effective.

Keywords: ecological fragmentation; maximum likelihood; landscape metrics and indices; Patch Analyst; IndiFrag; Ecuador



Citation: Rosero, C.; Otero, X.; Bravo, C.; Frey, C. Multitemporal Incidence of Landscape Fragmentation in a Protected Area of Central Andean Ecuador. *Land* **2023**, *12*, 500. <https://doi.org/10.3390/land12020500>

Academic Editors: María de la Cruz del Río-Rama, Amador Durán-Sánchez and José Álvarez-García

Received: 4 January 2023

Revised: 30 January 2023

Accepted: 4 February 2023

Published: 17 February 2023



Copyright: © 2023 by the authors. Licensee MDPI, Basel, Switzerland. This article is an open access article distributed under the terms and conditions of the Creative Commons Attribution (CC BY) license (<https://creativecommons.org/licenses/by/4.0/>).

1. Introduction

Approximately 80% of the planet has changed its natural conditions due to the incidence of anthropogenic activities [1]: humans and society have become a global geophysical force, what is called as Anthropocene [2] and naturally occurring factors [3], mainly because of changes in land cover and land use LULC [2,4,5]. Such changes are associated with environmental, socioeconomic, and political factors [6] that affect the landscape over time and space [3]. Mainly, the causes of land use change are the steady increase in population and the expansion of the agricultural frontier [6,7]. For example, the development of agriculture impacts water quality and the soil's ability to store carbon because of wastewater discharge, increasing the concentration of heavy metals and pesticides; these human activities also have altered the global cycle of N [8,9].

Regarding the consequences, LULC changes are the main factor causing climate change, water, soil, and air pollution [10], and loss of biodiversity and species habitat [1], modifying ecosystems at the biotic and abiotic levels [11–13]. Likewise, land use changes are one of the factors that most affect ecosystem services, as they alter the natural characteristics, processes, and components of ecosystems [14,15]. Other consequences include climate change, soil erosion, forest fragmentation, and increased natural disasters [6,16,17]. Therefore, knowing the rate of land cover change is essential to guide decision-making on natural resources [1] assertively, environmental management, and planning [10], as this allows qualitative and quantitative estimation of the changes generated by anthropogenic activities on the landscape [18–20].

Landscape fragmentation goes hand in hand with LULC changes, considering the landscape as a heterogeneous expanse of land formed by ecosystem–human interaction [21] and fragmentation as a continuous process of ecosystem degradation until small discontinuous areas are included [7,22]. Such processes are associated with anthropogenic activities' spatial and temporal dynamics [23], such as mining, agricultural frontier expansion, forest fires, urbanization, and illegal logging [24]. Its effects are habitat reduction, species isolation, soil erosion, and loss of cultural identity and biodiversity [24,25]. Landscape metrics can measure fragmentation, which caters to an area's vegetation cover and change over time [23]. These metrics reflect the relationship between land use and its ecological processes, making it possible to quantify the adverse effects of LULC changes on landscape ecology [10].

Human pressure on natural resources and concern for biodiversity conservation lead to the creation of new protected areas [26], whose environmental conditions require constant monitoring to ensure the preservation of the natural resources they protect [27]. The application of remote sensing is a practical and fast way to obtain, visualize and analyze spatial data [27]. Therefore, assessing the efficiency of protected areas is a key factor for sustainability. Thus, the conservation of ecosystems is vital, as they provide several services such as regulating water sources and regional climate patterns and carbon sequestration [28,29]. It is possible to classify ecosystem services into four categories: Provisioning services (raw materials); supporting services (nutrient cycling and ecological niches); regulating services (climate); and cultural services (spiritual values). Furthermore, the capacity of ecosystems to provide their services depends on ecosystem health and integrity and is threatened by anthropogenic factors, compromising their availability for present and future generations [30].

The results of these technologies help decision-making on the quality of life in environments modified by human activities [24], so it is necessary to precisely know the regions where LULC changes occur [25].

Based on the above, it is strongly recommended to apply remote sensing technologies to evaluate LULC changes and landscape fragmentation due to satellite images, and multitemporal analyses are considered an efficient and low-cost alternative tool [1], in addition to applying to areas of large extensions or remote and inaccessible zones [23], reducing research time and obtaining more updated maps [31].

Maintaining ecological integrity is globally acknowledged as a strategic goal, but there has yet to be a consensus on a practical and widely usable methodology to assess it; some studies propose a comprehensive approach to quantify regional ecosystem integrity based on FAIR data obtained using satellite remote sensing and image analysis. There are three variables considered central to this approach: normalized difference vegetation index (NDVI), at-satellite brightness temperature (BT), and vegetation surface heterogeneity (HG), corresponding to ecosystem integrity indicators exergy capture, biotic water flows, and abiotic heterogeneity [32]. Standardized regional maps can help develop predictive models of the transitional ecosystem dynamic, and facilitate boundary planning of protected areas to maximize management and conservation [33]. There are several methods for mapping land cover changes using remotely sensed data: conventional maximum likelihood classification; post-classification; image different components change-detection techniques; vegetative index differencing; post-classification change differencing; and multi-date unsupervised classification. Land cover can be determined by analyzing satellite and aerial imagery, but land use cannot be determined from satellite imagery. Land cover maps provide information to help managers best understand the current landscape. Land cover maps for several years are needed to see change over time [34].

Remote sensing has become an essential tool applicable to developing and understanding the global, physical processes affecting the earth [34], especially in protected areas such as Llanganates National Park, which is characterized by having a wide altitudinal range that varies between 1200 to 4638 masl, highly irregular topography, with steep, almost vertical, slopes where we can find immense rocky walls, lagoons and foothills

forests. According to preliminary analysis, the park has some areas with natural vegetation and others with disturbed vegetation, determining the presence of more than 800 species of vascular plants, including some rare and endemic to the region that had not been recorded before. In comparison, the fauna consists of 231 species of birds, 46 mammals, and 23 amphibians and reptiles [35]. Biodiversity inside PNL is invaluable because some studies carried out in recent years have allowed the description of new species, such as frogs of the genus *Pristimantis* (Strabomantide) [36,37], new species of plants of g. *Brunellia* (Brunelliaceae) [38], and species of fungus of the genus *Xylaria* [39]; moreover, this has determined the ample mammal richness existing in this protected area [40]. Pollen records also provide information (radiocarbon dates) that indicates that the local paramo vegetation was relatively stable with only minor fluctuations since the mid-Holocene. The paramo vegetation was characterized mainly by Asteraceae, Cyperaceae, and Poaceae. The regional lower mountain rainforest vegetation is primarily represented by Moraceae/Urticaceae, and the upper mountain rainforest by Melastomataceae, *Polylepis*, and *Weinmannia*. Between ca. 4100 to 2100 cal yr BP, paramo was the primary main vegetation type with a low presence of mountain rainforest, probably reflecting conditions; however, between ca. 2100 cal yr BP and the present, the proportion of paramo vegetation increased with a decreased occurrence of mountain rainforest, suggesting cooler and moister conditions [41].

We have chosen the protected area of the Llanganates National Park due to its relevance to the environment, and considering all the ecosystem services it provides. Subsequently, the predominant purpose of the current study has been to evaluate the land cover and land use changes from 1991 to 2016 (25 years) through remote sensing technologies and geographic information systems. Furthermore, we also measure the degree of fragmentation in this protected area by calculating landscape metrics and indices with the safeguard space database information for the conservation of biodiversity of the Parks, necessary for designing and implementing measures for correct LULC use.

2. Materials and Methods

2.1. Study Area

The study was conducted in the Llanganates National Park (PNL), a protected area in the central Andean region of Ecuador, coordinates 01°08' S and 78°14' W. It covers approximately 220,000 hectares and occupies certain areas of the Tungurahua, Napo, Cotopaxi, and Pastaza Provinces. Its altitudinal range goes from 1200 to 4638 masl. It was declared a protected area in 1996 due to its rich biodiversity and Ramsar sites of interest [11].

The study area was divided into three watersheds to emphasize the research's ecological purpose: the Pastaza, Yanayacu, and Jatunyacu rivers (Figure 1). The three watersheds share similar morphometric characteristics: their oblong shape derived from compactness indices more significant than 1.5, hypsometric curves with waterways in their juvenile stage, the terrain has a medium to steep slope (10-, low drainage density, high runoff time and an unstable flow regime).

2.2. Satellite Image Processing

Satellite images for this study were obtained from the U.S. Geological Survey website. Three 30-m resolution satellite images were used to cover a 25-year study period (from 1991 to 2016), with minimal cloud cover possible. For each date, a mosaic of the satellite images of continuous quadrants 60 and 61 covered the entire extent of the watersheds.

From the Landsat satellite, it was obtained following datasets with their respective acquisition dates: Landsat 5 Thematic Mapper (TM) (15 October 1991), Landsat 7 Enhanced Thematic Mapper (ETM+) (3 November 2001), Landsat 8 Operational and Land Imager (OLI) (20 November 2016), the Path row was 10–60 and 61, while the processing level was collection 2 Level 2 Imagery Products with a spatial resolution of 30 m USGS (2022). To improve The quality of satellite images and obtain better results in the classification phase [21,42], the radiometric and atmospheric correction was performed by applying the

parameters and procedures of the FLAASH method in the ENVI 5.3 software [43] Based on this, the Top-of-atmosphere reflectance (TOA) was obtained [27].

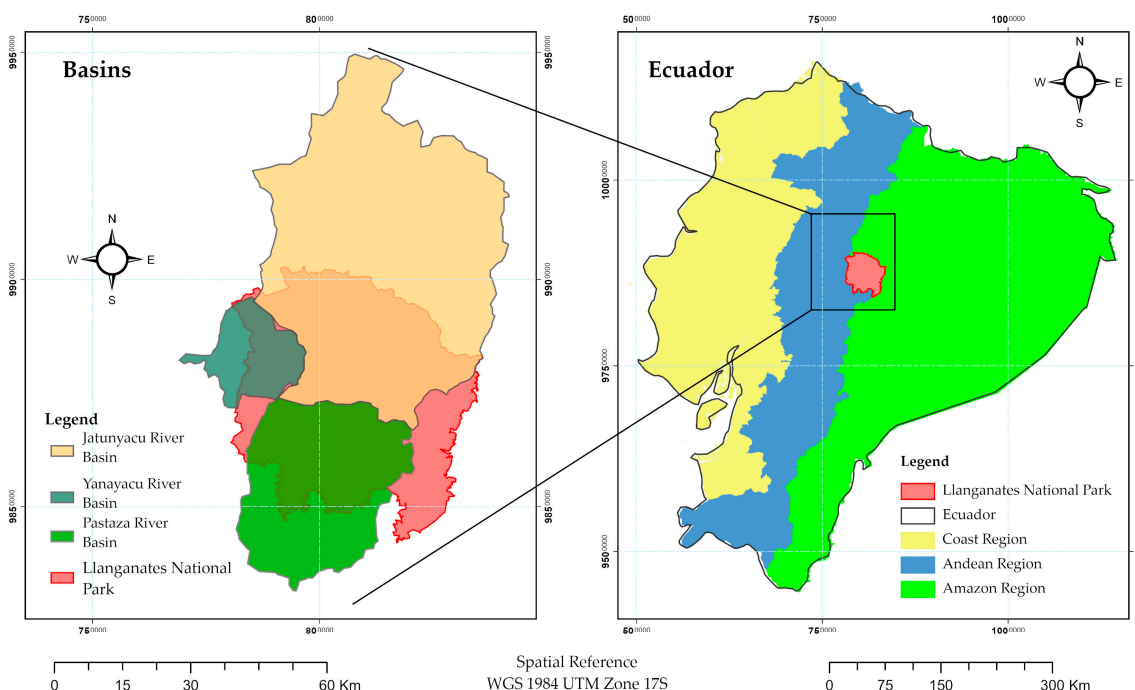


Figure 1. Location of the Llanganates National Park, Ecuador, with its four basins, Pastaza, Yanayacu, Jatunyacu, and Llanganates river.

2.3. Supervised Classification

To identify the land cover in the three watersheds associated with the PNL, the ecosystem classification system of Ecuador was used as the basis for this study; the following covers were recognized: (1) forest; (2) agricultural areas; (3) shrub and herbaceous vegetation (3.1) flooded grassland paramo, (3.2) grassland paramo; (4) water bodies; (5) anthropic areas; (6) areas without vegetation cover; (7) snow; and (8) no information—clouds.

Supervised classification is a data-driven (practical) modeling tool that derives statistical relationships between the input and the ground truth habitats [44]. A semantic classification of aerial/satellite images is essential for land cover and land use mapping, change detection, emergency response or management, and various other applications [45]. Conventional approaches to training a supervised image classification aim to describe all classes spectrally and fully. Therefore, extensive training is typically required to describe each feature space type comprehensively [46]. Supervised Classification methods usually give successful results with high overall accuracy for determining LULC studies [47]. These methods have been widely used to identify land cover [48] and require knowing the spectral attributes of the study area (in this study, the spectral characteristics were obtained by a Principal Component Analysis—PCA). Among the different supervised classification methods, Maximum Likelihood Classification is reported as the one with higher accuracy, good separation from classes [49] and the most common algorithm for LULC analysis [50].

The supervised classification was carried out with the maximum likelihood method that depends on Bayes' theorem and assumes that the data obey a Gaussian distribution [3,27]. It is based on a pixel analysis, where each pixel is assigned to the class with the highest likelihood according to its spectral distribution [3,27]. It is a simple and effective method, widely used in remote sensing due to its robustness and degree of sophistication [23,31,51].

The training phase for supervised classification consisted of selecting pixels representing known patterns based on knowledge of the study area [52]. Thus, the training zones were defined to ensure spectral separability of the classes and taking the most Homogeneous Regions of Interest (ROI), being revised and modified until reaching a

Jeffries–Matusita Distance as close as possible to two [27,53]. In addition, a 3 × 3 window majority filter was applied on the generated land cover map to reduce the “salt and pepper” effect and improve the resulting map’s visual quality [52].

2.4. Post Classification

Satellite image classification processes require the evaluation of accuracy as a fundamental part of the validation of results, defining the quality and significance of the results [53]. Therefore, a confusion matrix was constructed for each scenario with which the percentage of correctly classified pixels about the land covers present in the study area is visualized. In addition, the overall accuracy of the classification process was evaluated by calculating the non-parametric Kappa test. The acceptable value for land use change maps should be more excellent than 85% [3,31]. Its calculation is given by the equation [43]:

$$K = \frac{N \sum_{i=1}^r (x_{ii}) - \sum_{i=1}^r (x_{i+} * x_{+i})}{N^2 - \sum_{i=1}^r (x_{i+} * x_{+i})}$$

where: *N*: total number of observed pixels, *i* and *r*: number of rows in the confusion matrix, *x_{ii}*: number of observed pixels in row *i* and column *I*, *x_{i+}*: total number of marginal observations in row *i*, and *x_{+i}*: total number of marginal observations in column *i*. The overall map accuracy, given by the ENVI software, was also calculated.

2.5. Landscape Metrics and Indices

Landscape metrics give the configuration and structure of an ecosystem, the main ones being the number, size, and shape of patches in the different classes that compose the landscape [53]. Once the land covers for the study area were obtained, the files were imported into ArcGIS software. Next, the landscape metrics were generated using the fragmentation analysis extension Patch Analysis [23], a spatial analysis program for maps in vector format [53].

Landscape metrics were calculated to assess ecological fragmentation in the PNL, from which the number of patches, mean patch size and the coefficient of variance of patch size were selected for their respective analysis. It should be noted that the results of all landscape metrics will not be presented. Many were redundant and some did not apply to the study area, so only those considered appropriate to the landscape under analysis were selected [21]. The IndiFrag v2.1 software was also used to calculate some multitemporal indices described in Table 1.

Table 1. Selected landscape metrics and indices.

Landscape Metric	Description	Value Range	Reference
Mean Patch Size (MPS)	Average patch size.	MPS ≥ 0	[54]
Shannon’s Evenness Index (SEI) SEI = $\frac{-\sum_{i=1}^m (p * (\ln p))}{\ln m}$	The measure of patch distribution and abundance is based on several classes. m: number of classes. p: relation between class area and landscape area.	From zero (0) to one (1). 0: distribution of patches is low. One or near: distribution of classes is more even.	[54,55]
Rate of change (RC) RC = $\frac{1}{t_2 - t_1} * \ln \left(\frac{A_{t_2}}{A_{t_1}} \right) * 100$	Measure an overall area change in classes through time. It is expressed in percentage.	From (0) to 100%.	[55]
Expansion Index (LEI) LEI = $\frac{l_w}{P_w} * 100$	Measure of growing type: infilling, edge-expansive and outlying. l _w : shared perimeter length between new and former patch P _w : perimeter of new patch	From zero (0) to 100%.	[55]

In each period (1991–2001 and 2001–2016), the thematic maps and index values were compared to find the level of vegetation cover change [3].

3. Results

3.1. Land Cover Classification

During the training phase of the classification process, the separability of the classes for each scenario (for each watershed in each year) was determined, obtaining values above 1.6, which indicates that the courses have been correctly defined and there is no significant overlap in the spectral signatures [6]. However, there is a slight similarity in the reflectance of the classes: grassland paramo, flooded grassland paramo, agricultural areas, and anthropogenic zones (in particular, green areas spaces parks) because they have plant species in similar growth stages.

The satellite images were qualified in the ENVI software with the Maximum Likelihood method. Three land cover maps were obtained for each watershed corresponding to each year of study. Figure 2 shows the land covers found for the Jatunyacu (seven classes), Yanayacu (six courses), and Pastaza (eight classes) river basins.

The Jatunyacu River basin shows forest as the dominant cover that maintains a relatively constant area from 1991 to 2016. However, in 2016, the presence of clouds decreased the visibility of the surfaces, especially in the northern sector of the basin. The change from moorland flooded grassland to moorland grassland is also observed in both periods. The agricultural areas extend north of the basin over time, while the snow and water bodies do not change transparently. Areas without vegetation cover remain constant and are mainly associated with the slopes of the extinct active Antisana (northeast) and Cotopaxi (north) volcanoes [56,57].

In the Yanayacu River basin, it is observed that between 1991 and 2001 anthropogenic areas did not change significantly, while from 2001 to 2016, an increase in anthropogenic areas was noted in the west–east direction of the basin. Agricultural areas occupy a similar place in all years. Flooded grassland paramo increased from 1991 to 2001 but decreased slightly by 2016.

The most notable change in the cover is from flooded grassland paramo to grassland paramo and vice versa. There are very few discontinuously distributed forest patches in this watershed. Water bodies remain constant, the most important being the Pisayambo Lagoon and the Antejos Lagoons to the southeast of the basin.

The forest is the dominant cover in the Pastaza River basin, and there has been no considerable variation over the years. Agricultural areas roughly conserved their site from 1991 to 2001 and increased their size slightly until 2016. Anthropogenic regions are in the southwestern part of the watershed, and no evident variation is observed during the two periods. Areas without vegetation cover had the same area in 2001 but decreased in 2016, replaced by forest and grassland paramo cover. Very few patches of floodable grassland paramo and small size are distributed discontinuously in the northwestern part of the watershed. The water bodies remain constant over the years.

3.1.1. Confusion Matrix and Overall Accuracy

To verify the quality of the classification, the overall accuracy of the land cover map was calculated, and in parallel, the Kappa coefficient, using the ENVI 5.3 software. The results are presented in Table 2.

In general, the excellent quality of the classification is evidenced since it has high accuracy and precision with Kappa coefficients close to 1 and accuracy percentages more significant than 90%; this value is higher than the acceptable value (85%) established by [3]. With this, it is assumed that the defined classes and the classification method are suitable for the study area. On the other hand, the confusion matrix contains the number or percentage of pixels adequately classified according to the field land cover concerning those organized by the software [51]. For this study, a bar chart representing this percentage was chosen to improve the visualization of the data as they have been very extensive for the reader (Figure 3).

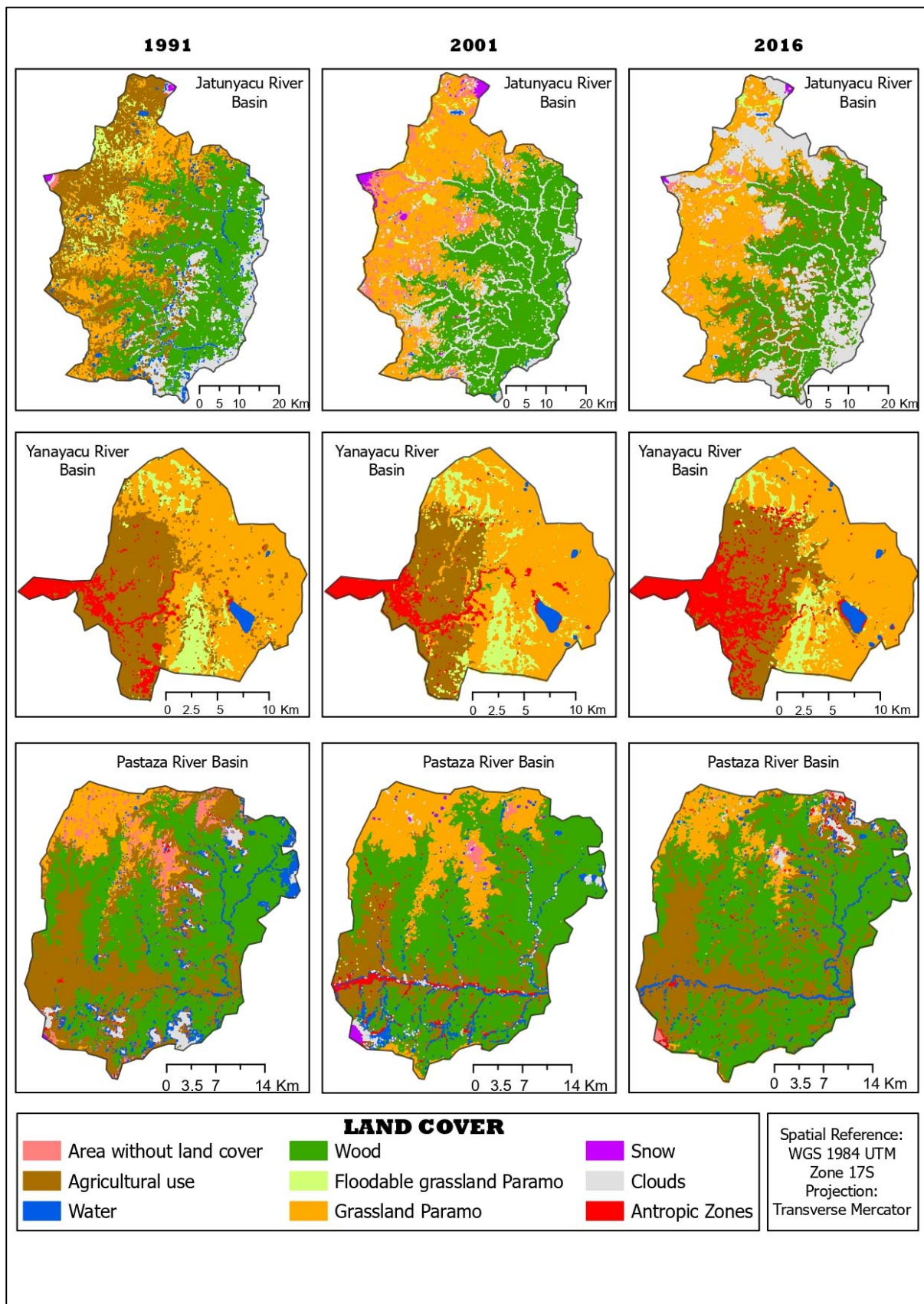


Figure 2. Geospatial distribution and land cover changes in the years 1991, 2001, and 2016 of three basins of the Llanganates National Park.

Table 2. Kappa (κ) coefficient and overall accuracy of the supervised classification.

	1991		2001		2016	
	Kappa Coefficient	Overall Accuracy (%)	Kappa Coefficient	Overall Accuracy (%)	Kappa Coefficient	Overall Accuracy (%)
Jatunyacu River Basin	0.95	96.00	0.91	92.69	0.92	95.23
Yanayacu River Basin	0.94	95.27	0.92	93.44	0.96	96.91
Pastaza River Basin	0.94	95.97	0.95	96.95	0.95	96.24

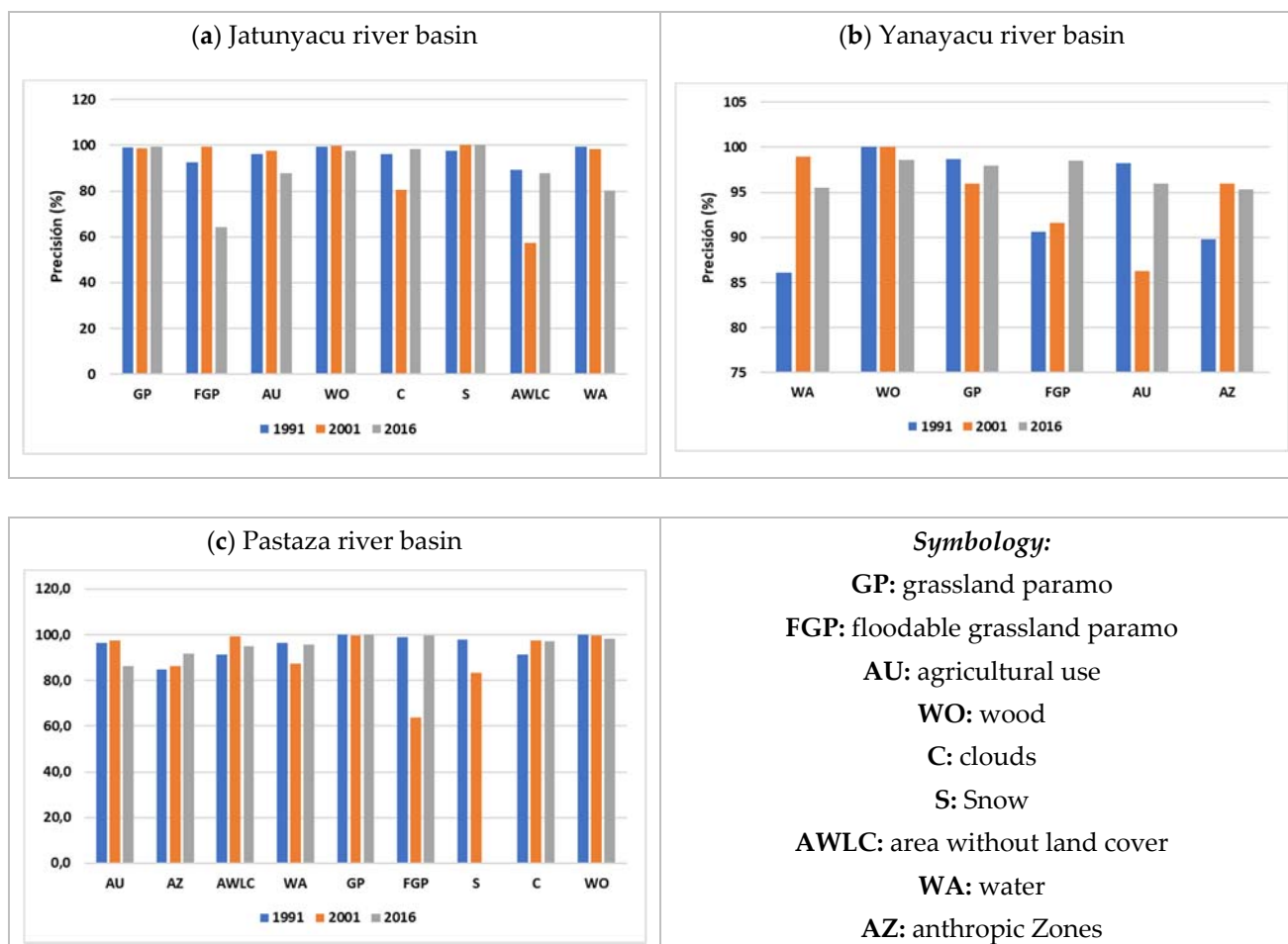


Figure 3. Modified confusion matrix for (a) Jatunyacu, (b) Yanayacu, and (c) Pastaza river basins.

From the modified confusion matrix, most image pixels were correctly classified, except for the flooded grassland paramo in 2016 areas without vegetation cover in 2001 within the Jatunyacu River basin and the flooded grassland paramo in 2001 within the Pastaza River basin. In the first case, the flooded grassland paramo was classified as agricultural areas, probably because the software erroneously interpreted the amount of irrigation water in the terrain instead of the flooding regime of the paramo. Something similar occurred with the areas without vegetation cover identified by the software as agricultural areas because the land used by farmers could have been left uncultivated during that month in 2001. Regarding the other land covers, it is observed that the accuracy of their classification is higher than 85%.

3.1.2. Landscape Metrics and Indices

Over time, the magnitude of ecosystem modifications is measured through landscape metrics and fragmentation indices. The mean patch size for each watershed is presented in Figure 4.

In Figure 4a the forest patch size was more prominent in 2001. However, this does not necessarily mean that there has been a growth in the area of this cover since, with the help of the coverage map, it is observed that a significant number of clouds covered the study area in 1991 and 2016, reducing the interpretation of the software concerning the terrain in reality. Something similar occurs with the snow and grassland cover, which is also affected in its visibility by the layer of clouds covering the area. In the case of water bodies, the most extensive is the “Laguna de la Mica”, located in the northern part of the basin on the slopes of snowy Antisana, progressively increasing its extension from 1991 to 2016. Concerning the coverages, the variation in patch size is narrow.

In the Yanayacu River basin it is observed that the flooded grassland paramo had a high total class area/number of patches ratio in 1991, which decreased in 2001 and increased slightly in 2016. This may be because initially, the extent of this cover is less extensive. Still, there are few large patches, while in 2001 the volume increased and the number of patches increased, decreasing the ratio. In addition, there is approximately the same extent in 2016 as in 2001, but fewer patches. The other land covers have a similar mean patch size in all years with proportional variations in the number and area of patches.

In the Pastaza River basin, the interference generated by clouds on the mean forest patch size is slightly noticeable, mainly because its extension is similar in the three years. Still, the number of patches varies, causing this parameter to go from one year to another. Regarding snow, it was found that in 1991 the snow patches to a certain extent; in 2001, the volume increased, and the patches decreased, but in 2016, the snow disappeared utterly. The areas without vegetation covered several patches in 1991 to a more significant extent causing a low value of mean patch, which increased in 2001 due to the decrease in the number and area of patches, decreasing even more by 2016. These areas were replaced by grassland paramo and forest cover. The other coverages show a slight variation concerning this landscape metric.

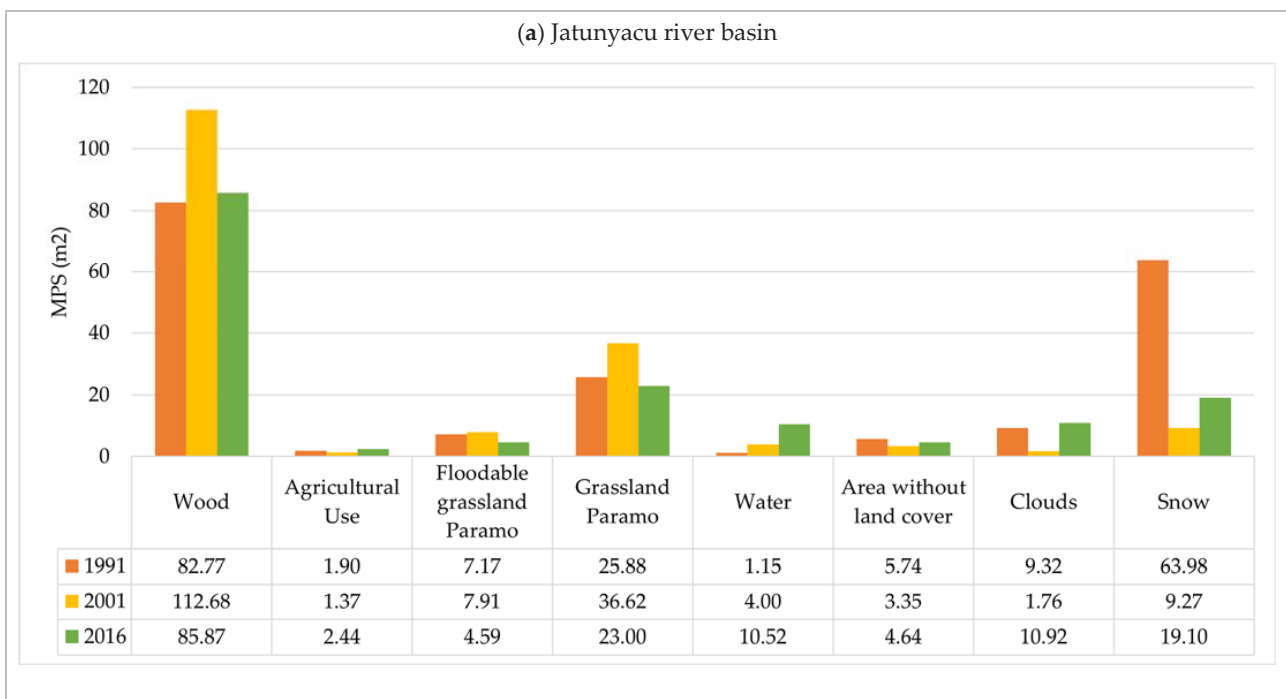


Figure 4. Cont.



Figure 4. Average patch size classes for each river basin.

To more clearly and numerically evidence the changes that occurred in the three watersheds associated with the PNL, the change ratio expressed in percentage and the land cover expansion index were calculated for the two study periods (1991 to 2001 and 2001 to 2016), as listed in Tables 3–5.

The forest, grassland paramo, snow, and areas without vegetation cover increased in the first period. In contrast, agricultural zones, water, and floodable grassland paramo cover decreased (negative sign) by 2 to 6%. The growth of areas without vegetation cover has been mostly isolated, i.e., patches of different sizes were formed in 2001 in sites utterly separate from the continuous patches present in 1991. The growth of the forest has been filling because the clouds in the center of the forest in 1991 were not present in 2001, leaving the natural ground cover visible. The grassland paramo had a filler type of growth because

there were areas of different surfaces surrounded by this cover that were modified to grassland paramo. In the case of snow, it had an expansive type of growth; that is to say, the area of increase in the cover was continuous concerning the extension that existed initially. In the second period, only the agricultural areas increased their expansion with an expansive type of growth, living; in 2016, new plots of crops continued to those existing in 2001. At the same time, the rest of the coverages decrease between (>) 0 to 12%.

Table 3. Rate of change and expansion index: Jatunyacu River Basin.

Period: 1991 to 2001				
Classes	RC (%)	Expansion Index (LEI) km ² /Year and Percentage		
		Infilling	Edge-Expansive	Outlying
Area without land cover	4.28	0.30 (10.28%)	1.11 (37.50%)	1.54 (52.22%)
Agricultural Use	−6.51	0.32 (6.88%)	2.81 (59.74%)	1.57 (33.38%)
Water	−2.85	0.00 (0.39%)	0.24 (64.72%)	0.13 (34.89%)
Wood	0.84	13.81 (72.93%)	4.92 (25.96%)	0.21 (1.11%)
Floodable grassland Paramo	−3.33	1.29 (45.84%)	1.32 (46.95%)	0.20 (7.21%)
Grassland Paramo	1.29	10.57 (58.49%)	6.92 (38.32%)	0.58 (3.19%)
Snow	6.39	0.00 (0.24%)	0.55 (80.46%)	0.13 (19.29%)
Period: 2001 to 2016				
Area without land cover	−7.99	0.06 (14.94%)	0.26 (61.53%)	0.10 (23.54%)
Agricultural Use	8.26	0.55 (3.04%)	11.41 (63.22%)	6.09 (33.73%)
Water	−4.59	0 (0%)	0 (100%)	0 (0%)
Wood	−0.28	2.66 (35.93%)	3.59 (48.47%)	1.16 (15.59%)
Floodable grassland Paramo	−7.44	0.15 (24.90%)	0.32 (52.52%)	0.14 (22.58%)
Grassland Paramo	−2.48	2.86 (66.75%)	1.30 (30.34%)	0.12 (2.91%)
Snow	−11.79	0.01 (1.24%)	0.64 (79.51%)	0.15 (19.25%)

For the Yanayacu river basin, the results presented in Table 4 were obtained.

In the first period, agricultural areas, forests, and moorland flooded grassland, and anthropogenic zones increased between 1 and 10%. Water and grassland paramo decreased between 1 and 4%. Agricultural areas and flooded grassland paramo had an expansive type of growth. The forest and the anthropic regions had an isolated change. In the second period, agricultural areas, water, and anthropic zones grew between 0.5 and 5%. All these coverages presented an expansive type of growth. Forest cover and the two types of grasslands decreased between 0.6 and 11%. For the Pastaza river basin, the results are presented in Table 5.

Table 4. Rate of change and expansion index: Yanayacu River Basin.

Period: 1991 to 2001				
Classes	RC (%)	Expansion Index (LEI) km ² /Year and Percentage		
		Infilling	Edge-Expansive	Outlying
Agricultural Use	1.48	0.87 (31.43%)	1.41 (50.82%)	0.49 (17.75%)
Water	−1.51	0.0002 (7.96%)	0.0016 (75.30%)	0.0004 (16.73%)
Wood	10.55	0.04 (7.13%)	0.20 (39.45%)	0.27 (53.42%)
Floodable grassland Paramo	9.53	0.35 (8.13%)	2.88 (66.40%)	1.10 (25.46%)
Grassland Paramo	−3.72	0.17 (45.88%)	0.15 (40.13%)	0.05 (14.00%)
Antropic Zones	1.43	0 (0%)	0 (0%)	1.63 (100%)
Period: 2001 to 2016				
Agricultural Use	1.10	0.42 (14.05%)	2.23 (74.36%)	0.35 (11.59%)
Water	0.53	0.0015 (5.67%)	0.02 (92.74%)	0.0004 (1.59%)
Wood	−10.79	0.0001 (1.67%)	0.0040 (55.72%)	0.0031 (42.61%)
Floodable grassland Paramo	−2.65	0.13 (25.85%)	0.29 (59.08%)	0.07 (15.06%)
Grassland Paramo	−0.60	0.82 (51.73%)	0.73 (45.61%)	0.04 (2.66%)
Antropic Zones	4.78	0.33 (25.32%)	0.61 (46.76%)	0.36 (27.93%)

In the first period, the forest, moor grassland, snow, and anthropic zones increased their extension by 0.5 to 15%. The growth of the forest has been of the filling type, the moor grassland and snow have been of the expansive type, and the anthropic zones of the isolated type. On the other hand, the areas without vegetation cover, agricultural and livestock areas, water, and flooded moor grassland decreased in size by 2 to 22%.

In the second period, agricultural areas, moorland flooded grassland, moorland grassland, and the anthropic regions increased their extension by 0.3 to 4%. The growth of the farming areas was expansive, the floodable grassland paramo and the anthropic zones had an isolated type of growth, and the moorland grassland had an infill type of growth. Areas without vegetation cover, water, and forest reduced in extent by 0.5 to 5%. Snow is recorded as no data because the formulas cannot be applied for a cover with 0 km² area since this cover disappeared entirely from 2001 to 2016.

Finally, the Shannon Uniformity index was calculated, the results of which are presented in Figure 5.

Table 5. Rate of change and expansion index: Pastaza river basin.

Period: 1991 to 2001				
Classes	RC (%)	Expansion Index (LEI) km ² /Year and Percentage		
		Infilling	Edge-Expansive	Outlying
Area without land cover	−12.91	0.02 (21.02%)	0.08 (75.00%)	0.0042 (3.97%)
Agricultural Use	−2.46	0.67 (20.30%)	1.70 (51.67%)	0.92 (28.03%)
Water	−7.31	0.03 (2.60%)	0.64 (58.72%)	0.42 (38.68%)
Wood	1.47	10.08 (70.76%)	3.69 (25.92%)	0.47 (3.32%)
Floodable grassland Paramo	−22.34	0.0001 (1.05%)	0.0008 (9.43%)	0.0076 (89.52%)
Grassland Paramo	0.70	1.35 (42.58%)	1.62 (51.05%)	0.20 (6.38%)
Snow	13.71	0 (0%)	0.21 (85.00%)	0.04 (15.00%)
Antropic Zones	1.51	0.03 (6.09%)	0.14 (33.09%)	0.27 (60.83%)
Period: 2001 to 2016				
Area without land cover	−0.66	0.0001 (0.04%)	0.03 (10.79%)	0.28 (89.17%)
Agricultural Use	1.81	0.87 (18.40%)	2.55 (53.96%)	1.31 (27.65%)
Water	−5.08	0.01 (5.07%)	0.09 (33.96%)	0.17 (60.96%)
Wood	−0.54	1.19 (56.11%)	0.84 (39.41%)	0.096 (4.48%)
Floodable grassland Paramo	2.18	0 (0.00%)	0 (0%)	0.0088 (100.00%)
Grassland Paramo	0.37	0.83 (45.14%)	0.69 (37.17%)	0.33 (17.69%)
Snow	No Data	No Data	No Data	No Data
Antropic Zones	3.76	0 (0%)	0 (0%)	0.75 (100.00%)

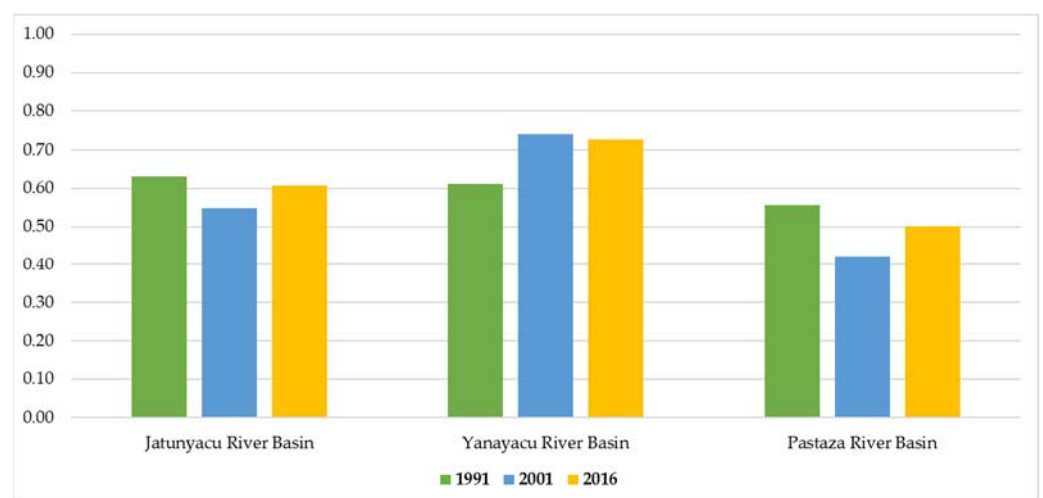


Figure 5. Shannon's Evenness Index (USHAN) for each basin.

According to the graph, the three watersheds show a uniform distribution of biodiversity since the SEI values are far from zero (0) and close to one (1). In addition, there is a slight noticeable variation over time. The Yanayacu River basin has the highest SEI values; therefore, its biodiversity is possibly high and more-evenly distributed than the other basins.

3.1.3. Statistical Analysis

From the data on the number of patches present in each watershed, a statistical analysis was applied to test for significant differences in the land covers of the three watersheds associated with the PNL. Similarly, the standard deviation of patch size was used to measure variability to find discrepancies between land covers within the study period (1991 to 2016). Regarding the first question, the result was a frequency histogram (Figure 6) showing many small-sized patches with a high frequency in the three watersheds that make up the Llanganates National Park. This, in turn, is attributed to the fact that the patches are homogeneously distributed throughout the study area.

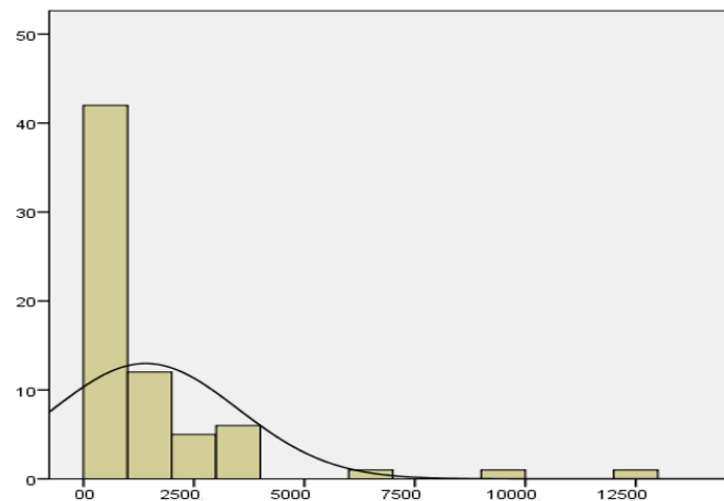


Figure 6. Frequency histogram for the number of patches in the three basins. Median = 1407.15; Standard deviation = 2090.339; N = 68.

Based on the evident leftward bias in the frequency histogram of the number of patches, the Kruskal–Wallis nonparametric test for independent samples was performed with a significance level of 0.05. The trial resulted in a p -value of 0.001, which is less than the significance level and allows us to interpret that there is a significant difference between the ecosystems present in some of the three watersheds associated with the PNL.

After verifying the difference between the watersheds, a multiple-range test was performed, finding that the Yanayacu River watershed has a significant difference from the Jatunyacu River watershed, and that there is no significant difference concerning the Pastaza River watershed. The differences between the basins are because each basin has its extension and specific land covers, in addition to the fact that these are distributed differently. Continuing with the second question, a histogram of frequencies of the patch size standard deviation (PSSD) was made for each year of study in each of the watersheds. The results are presented in Figure 7.

In Figure 7 the non-parametric Kruskal–Wallis multiple range test was applied, it can be interpreted that during the study period, from 1991 to 2016, there is no significant difference in patch size for the three watersheds, i.e., land covers do not vary significantly over time.

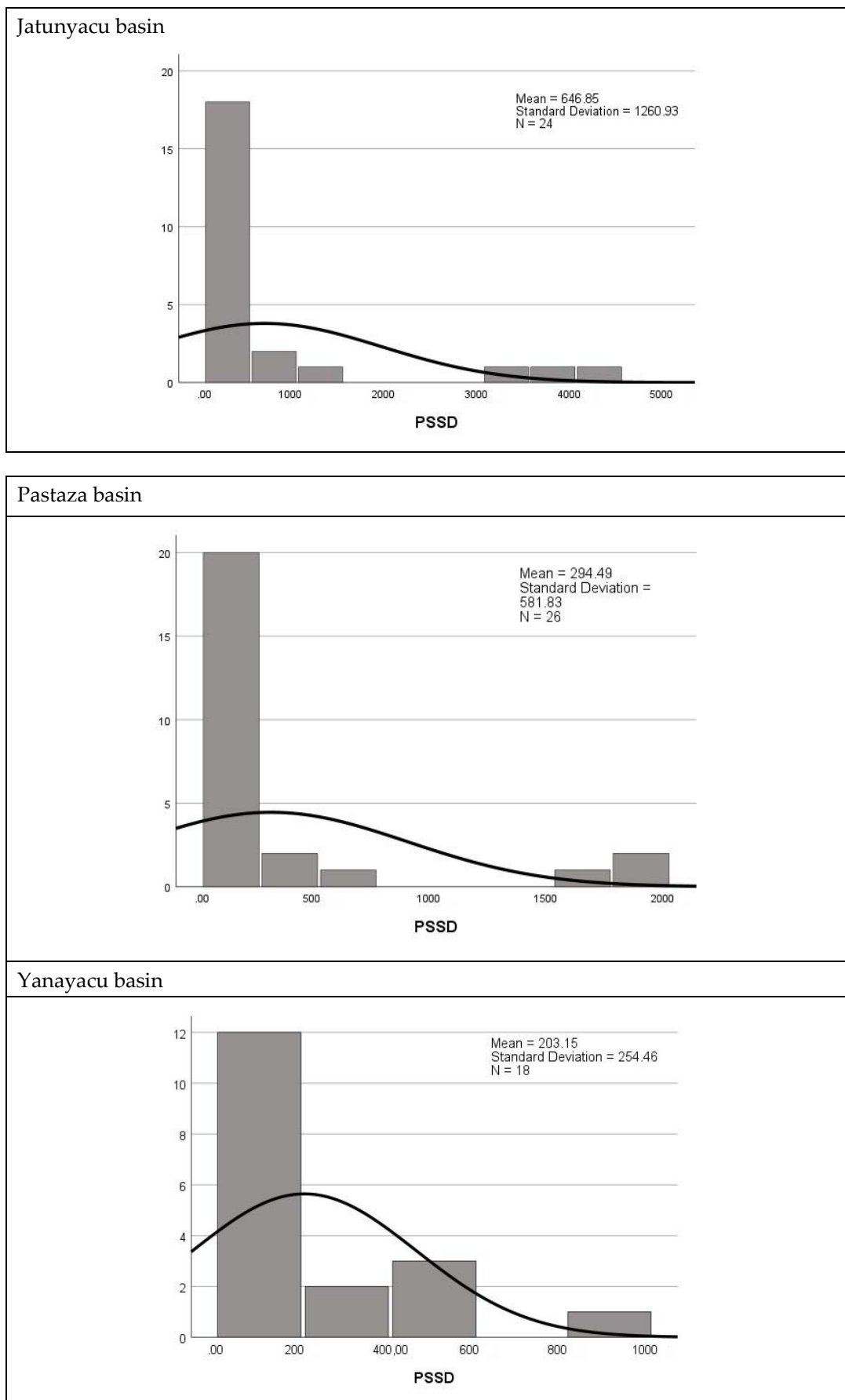


Figure 7. Histograms of PSSD frequencies for each basin.

4. Discussion

The analysis of land cover changes using the map and landscape metrics showed that these changes are insignificant. It is also worth mentioning that the most “abrupt” changes within the three watersheds occur in most cases outside of the protected area boundaries. For example, agricultural areas increased in all three watersheds due to the conversion of forest land or land with shrub and herbaceous cover to agrarian land because of population increase and the constant food demand that occurs in Ecuador and worldwide [1,58]. The Jatunyacu River basin was in the northern sector, the Yanayacu River basin in the western sector and the Pastaza River basin in the central~southern sector. However, there was a slight increase in anthropogenic zones in the Yanayacu and Pastaza river basins, showing the urban expansion in the region.

The dynamism of vegetation cover is typical of ecosystems and their volatility. A study in China presents similar results to the present research: changes in land cover and land use affect the entire territory, and the volatility of these changes overlap in specific extensions of the protected areas of this country; this does not necessarily mean that there is a deficiency in the ecosystem protection system of the protected areas, but rather that they present a natural dynamism over the years [59].

There is also a similar trend in land cover change in different parts of the world: in the Yellow River Basin (YRB), China, urbanized areas grew by 15 to 26% in a decade, compared to the study area that grew by 1.4 to 4.8% per year. Moreover, forests in YRB and the study area have varied dynamics over the decades, expanding and decreasing without a fixed trend, grasslands decrease, and other natural areas such as water bodies and deserts (in YRB) reduce and increase in a non-predictive way [60]. Similar results were also found in South Africa [21] and Cambodia [52].

Another aspect of the land cover maps is the clear presence of dominant land covers, such as the forest in the Jatunyacu and Pastaza River basins and the two types of paramo grasslands in the Yanayacu River basin [61]. This factor is vital because the predominance of one vegetation cover may indicate a low level of fragmentation in the study area [53]. In addition, a medium level of fragmentation can be attributed to the forest cover in the Yanayacu River basin because its patches are small and isolated on most occasions, creating the possibility that in the long term, this cover will disappear [62]. Something similar occurs with the paramo-flooded grassland in the Pastaza River basin, which has tiny and distant patches. A notable annotation is that the land covers in the three watersheds present medium to large extensions and tend to be continuous, indirectly indicating that the edges and shape of the patches are not complex, which helps to reduce the possible adverse effects of localized fragmentation processes that could occur in the study area [62].

Since there is low or no fragmentation in the protected area, it is possible to intuit the efficiency of protection and conservation of ecosystems and biodiversity at the local scale, which is high. It is relevant that Andean ecosystems are being protected, as they provide water and energy to specific populations, making it necessary to find strategies (declaration of new protected areas in critical conservation sites) to reduce the impact of human activities [12,29]. Landscape fragmentation implies the disruption of continuity, connectivity, and ecological functionality, decreasing the ability of species to move to other landscapes and endangering their survival [63]. On the contrary, in the study area, there are continuous patches of large extensions, which ensure that connectivity is recovered, except for the forest cover in the Yanayacu River basin and the flooded paramo grassland in the Pastaza River basin.

From the post-classification phase, relatively good quality of the process was obtained, which is vital. Currently, the accuracy of land cover classification processes has gained importance in the field of climate change, significantly contributing to efforts to control and mitigate this problem [3]. The landscape metrics and calculated indices allowed observing the study area’s spatiotemporal dynamics of land covers, noting that both natural and anthropogenic factors cause a medium dynamism. However, the changes are insignificant to the point of inducing landscape fragmentation processes. These parameters closely relate

to ecosystem services' quality, quantity, and distribution [25] Thus, ecosystem services in the study area are not strongly affected as there is low or no degree of fragmentation in the landscape and long and continuous habitats [63].

A study in Ghana recognized the potential adverse effects of soil changes on ecosystem services. However, they also state that adopting sustainable agricultural practices is critical to reducing soil degradation and meeting the food demand of the population [21] Therefore, it is essential to exempt protected areas from these changes and adopt a land use planning policy appropriate to the study region. It will fulfill two main objectives: the conservation of ecosystems and the sustainable satisfaction of human needs.

Another relevant study was conducted in Ethiopia, where four possible scenarios of LULC changes affecting ecosystem services were analyzed. The scenario related to ecosystem protection and agricultural development suggests a sustainable integration between these aspects. For this case, it was found that by 2051 the value of ecosystem services would amount to 960.5 million USD, being one of the most efficient ways to apply as a governance policy [58]. However, these land cover changes can also affect the water sources of a watershed in aspects such as runoff, infiltration, and water quality at different scales [64] For example, in the Yanayacu River basin, agricultural areas are advancing towards the central zone of the bay, getting dangerously close to the largest and most important body of water, the "Laguna de Pisayambo," which could cause water contamination. Therefore, sustainable management of the watershed concerning the direction of growth of this cover is vital for conserving water quality.

These effects are also reported by Sugianto et al. 2022 [65] in their research on Sumatra Island (Indonesia), where the analysis of LULC changes and their impact on the water variables of percolation, infiltration, and groundwater recharge was carried out. These effects occur because anthropogenic and natural activities can modify soil structure [66]. In contrast to the PNL watersheds, the Krueng Teunom watershed showed a high level of degradation and significant changes in land covers, which led to the conclusion that vegetation plays a vital role in water discharge, as watersheds with little vegetation discharge water quickly and suddenly, leading to flooding, the effect of which is enhanced by high slopes [65].

Concerning Shannon's Uniformity Index, biodiversity in the three watersheds is homogeneously or uniformly distributed throughout the land they occupy. Being an efficient, protected area, the values do not change significantly over time, thus contributing to the conservation of biodiversity and ecosystems [67]. In the study by [59], USHAN values in the range of 0.65 to 0.73 are obtained, interpreted as high biodiversity. Consequently, the area of interest in this study, with values of 0.4 to 0.7, has medium to increased biodiversity, with the Pastaza River Basin having the lowest biodiversity of the three studied.

Lastly, the analysis allows us to highlight the importance of watersheds for properly managing protected areas. This contributes to maintaining ecological integrity, biodiversity, and ecosystems [68,69]. Likewise, Ref. [70] mentions that the cost-benefit of repairing an ecosystem is much higher than conserving it from the early stages, for which establishing protected areas is fundamental. Saving the Ecuadorian Andes is accurate as it is a megadiverse country that suffered from deforestation and expansion of the agricultural frontier in vulnerable regions such as the paramos [41]. However, the present is different due to the study area selected still having the opportunity of being well managed; a study carried out in three various PAs in Tehran Province, namely Lar National Park, Jajrud PA, and TangehVashi National Natural Monument, has presented severe LULC changes and uncontrolled development of human activities [71]. We can also compare it with some studies carried out in such coastal ecosystems as Gorgan Bay and Gomishan Wetland, known as unique ecosystems in the south-eastern part of the Caspian Sea. This study demonstrated periodic changes in these ecosystems and the data over a period of 40 years, also using Landsat satellite imagery from 1978–2018. MSS, TM, and OLI imagery along with NDWI index. In general, remote sensing was an efficient tool for monitoring and managing ecosystems [72].

5. Conclusions

Once the level of fragmentation in the study area is almost zero or low, it can be concluded that the protected area of Llanganates National Park is actively fulfilling its mission, since the vegetation cover is maintained over time throughout the entire protected area, leaving the most accentuated changes outside its limits, especially those related to the increase in agricultural and livestock areas and anthropogenic zones. Since it is a protected area, the LULC changes were insignificant in the 25 years of the study. However, these have contributed to understanding the dynamism of natural and anthropogenic factors in the PNL. However, strategies must be implemented to prevent agricultural and urban expansion outside the PNL from entering the protected area and disrupting its natural balance.

On the other hand, several factors can affect the conservation effectiveness of a protected area; constant control and monitoring are essential to preserving the ecosystems and their biodiversity. It should be noted that it is necessary to include ecosystem services as a secondary axis of conservation, considering that they are affected by LULC changes and represent an opportunity to achieve sustainable management of watersheds and protected areas. Currently, the accuracy of land cover classification processes has gained importance in the field of climate change, significantly contributing to efforts to control and mitigate this problem.

Lastly, the analysis allows us to highlight the importance of watersheds for properly managing protected areas. Although this aspect contributes to maintaining ecological integrity, biodiversity, and ecosystems, the cost–benefit of repairing an ecosystem is much higher than conserving it from the early stages, for which establishing protected areas is fundamental—in particular, saving the Ecuadorian Andes due to it being a mega-diverse country, which for many years suffered from deforestation and expansion of the agricultural frontier in vulnerable areas such as the paramos. For example, at the Yanayacu river basin, agricultural areas are advancing towards the central zone of the basin, getting dangerously close to the largest and most important body of water, “Laguna de Pisayambo,” which could cause water contamination. Therefore, sustainable management of the watershed concerning the direction of growth of this coverage is vital for conserving water quality.

Author Contributions: Conceptualization, C.B. and C.R.; methodology, C.B., C.R. and X.O.; software, C.B.; validation, C.B., C.R. and X.O.; formal analysis, C.B.; investigation, C.B., C.R. and X.O.; resources, C.B. and C.R.; data curation, C.B. and C.R.; writing—original draft preparation, C.B.; writing—review and editing, C.F.; visualization, C.B.; supervision, C.R. and X.O.; project administration, C.R. and C.F.; funding acquisition, C.R. and C.F. All authors have read and agreed to the published version of the manuscript.

Funding: This research received no external funding.

Data Availability Statement: Data supporting reported results can be found in this personal repository: Land—Multitemporal Incidence of Landscape Fragmentation in a Protected Area of Central Andean Ecuador. https://livespochedu-my.sharepoint.com/:f/g/personal/cinthya_bravo_espoch_edu_ec/EmIA_wgbnnhFqqavNh4bVYABg0CbmbPxKs3HIgv5xEVhXQ (accessed on 3 January 2023).

Conflicts of Interest: The authors declare no conflict of interest.

References

1. Abdullah, H.M.; Islam, I.; Miah, G.; Ahmed, Z. Quantifying the spatiotemporal patterns of forest degradation in a fragmented, rapidly urbanizing landscape: A case study of Gazipur, Bangladesh. *Remote Sens. Appl. Soc. Environ.* **2019**, *13*, 457–465. [CrossRef]
2. Steffen, W.; Crutzen, P.J.; McNeill, J.R. The Anthropocene: Are humans now overwhelming the great forces of Nature. *AMBIO J. Hum. Environ.* **2007**, *36*, 614–621. [CrossRef]
3. Allam, M.; Bakr, N.; Elbably, W. Multi-temporal assessment of land use/land cover change in arid region based on landsat satellite imagery: Case study in Fayoum Region, Egypt. *Remote Sens. Appl. Soc. Environ.* **2019**, *14*, 8–19. [CrossRef]
4. Gao, J.; Li, F.; Gao, H.; Zhou, C.; Zhang, X. The impact of land-use change on water-related ecosystem services: A study of the Guishui River Basin, Beijing, China. *J. Clean. Prod.* **2017**, *163*, S148–S155. [CrossRef]

5. Vitousek, P.M.; Aber, J.D.; Howarth, R.W.; Likens, G.E.; Matson, P.A.; Schindler, D.W.; Schlesinger, W.H.; Tilman, D.G. Human alteration of the global nitrogen cycle: Sources and consequences. *Ecol. Appl.* **1997**, *7*, 737–750. [[CrossRef](#)]
6. Birhanu, L.; Hailu, B.T.; Bekele, T.; Demissew, S. Land use/land cover change along elevation and slope gradient in highlands of Ethiopia. *Remote Sens. Appl. Soc. Environ.* **2019**, *16*, 100260. [[CrossRef](#)]
7. Nkeki, F.N. Spatio-temporal analysis of land use transition and urban growth characterization in Benin metropolitan region, Nigeria. *Remote Sens. Appl. Soc. Environ.* **2016**, *4*, 119–137. [[CrossRef](#)]
8. Love, B.J.; Nejadhashemi, A.P. Water quality impact assessment of large-scale biofuel crops expansion in agricultural regions of Michigan. *Biomass Bioenergy* **2011**, *35*, 2200–2216. [[CrossRef](#)]
9. Turner, R.E.; Rabalais, N.N. Linking landscape and water quality in the Mississippi River Basin for 200 years. *BioScience* **2003**, *53*, 563–572. [[CrossRef](#)]
10. Japelaghi, M.; Gholamalifard, M.; Shayesteh, K. Spatio-temporal analysis and prediction of landscape patterns and change processes in the Central Zagros region, Iran. *Remote Sens. Appl. Soc. Environ.* **2019**, *15*, 100244. [[CrossRef](#)]
11. Gomez-Casanovas, N.; Matamala, R.; Cook, D.R.; Gonzalez-Meler, M.A. Net ecosystem exchange modifies the relationship between the autotrophic and heterotrophic components of soil respiration with abiotic factors in prairie grasslands. *Glob. Chang. Biol.* **2012**, *18*, 2532–2545. [[CrossRef](#)]
12. Mendoza, S.J.E.; Etter, R.A. Multitemporal analysis (1940–1996) of land cover changes in the southwestern Bogotá highplain (Colombia). *Landsc. Urban Plan.* **2002**, *59*, 147–158. [[CrossRef](#)]
13. Zhou, T.; Zhang, J.; Qin, Y.; Jiang, M.; Qiao, X. The Effects of Biotic and Abiotic Factors on the Community Dynamics in a Mountain Subtropical Forest. *Forests* **2021**, *12*, 427. [[CrossRef](#)]
14. Cayambe, J.; Torres, B.; Cabrera, F.; Díaz-Ambrona, C.G.H.; Toulkeridis, T.; Heredia-R, M. *Changes of Land Use and Land Cover in Hotspots within the Western Amazon: The Case of the Yasuní Biosphere Reserve*; Springer: Berlin/Heidelberg, Germany, 2023; pp. 213–223. [[CrossRef](#)]
15. Heredia-R, M.; Cayambe, J.; Schorsch, C.; Toulkeridis, T.; Barreto, D.; Poma, P.; Villegas, G. Multitemporal Analysis as a Non-Invasive Technology Indicates a Rapid Change in Land Use in the Amazon: The Case of the ITT Oil Block. *Environments* **2021**, *8*, 139. [[CrossRef](#)]
16. Parmesan, C. Ecological and Evolutionary Responses to Recent Climate Change. *Annu. Rev. Ecol. Evol. Syst.* **2006**, *37*, 637–669. [[CrossRef](#)]
17. Toulkeridis, T.; Zach, I. Wind directions of volcanic ash-charged clouds in Ecuador—Implications for the public and flight safety. *Geomat. Nat. Hazards Risk* **2016**, *8*, 242–256. [[CrossRef](#)]
18. Du, P.; Li, X.; Cao, W.; Luo, Y.; Zhang, H. Monitoring urban land cover and vegetation change by multi-temporal remote sensing information. *Min. Sci. Technol.* **2010**, *20*, 922–932. [[CrossRef](#)]
19. Hua, L.; Shao, G.; Zhao, J. A concise review of ecological risk assessment for urban ecosystem application associated with rapid urbanization processes. *Int. J. Sustain. Dev. World Ecol.* **2016**, *24*, 248–261. [[CrossRef](#)]
20. Roy, A. Land Use and Land Cover Change in India: A Remote Sensing & GIS Perspective. 2010. Available online: <https://www.researchgate.net/publication/289770159> (accessed on 3 January 2023).
21. Kankam, S.; Osman, A.; Inkoom, J.N.; Fürst, C. Implications of Spatio-Temporal Land Use/Cover Changes for Ecosystem Services Supply in the Coastal Landscapes of Southwestern Ghana, West Africa. *Land* **2022**, *11*, 1408. [[CrossRef](#)]
22. Shimrah, T.; Sarma, K.; Varga, O.G.; Szilard, S.; Singh, S.K. Quantitative assessment of landscape transformation using earth observation datasets in Shirui Hill of Manipur, India. *Remote Sens. Appl. Soc. Environ.* **2019**, *15*, 100237. [[CrossRef](#)]
23. de León Mata, G.D.; Pinedo Álvarez, A.; Martínez Guerrero, J.H. Application of remote sensing in the analysis of landscape fragmentation in Cuchillas de la Zarca, Mexico. *Investig. Geogr.* **2014**, *84*. [[CrossRef](#)]
24. Murad, C.A.; Pearse, J. Landsat study of deforestation in the Amazon region of Colombia: Departments of Caquetá and Putumayo. *Remote Sens. Appl. Soc. Environ.* **2018**, *11*, 161–171. [[CrossRef](#)]
25. Mugiraneza, T.; Ban, Y.; Haas, J. Urban land cover dynamics and their impact on ecosystem services in Kigali, Rwanda using multi-temporal Landsat data. *Remote Sens. Appl. Soc. Environ.* **2018**, *13*, 234–246. [[CrossRef](#)]
26. Reddy, C.S.; Saranya, K.; Jha, C.; Dadhwal, V.; Murthy, Y.K. Earth observation data for habitat monitoring in protected areas of India. *Remote Sens. Appl. Soc. Environ.* **2017**, *8*, 114–125. [[CrossRef](#)]
27. Belenok, V.; Noszczyk, T.; Hebryn-Baidy, L.; Kryachok, S. Investigating anthropogenically transformed landscapes with remote sensing. *Remote Sens. Appl. Soc. Environ.* **2021**, *24*, 100635. [[CrossRef](#)]
28. Foley, J.A.; Asner, G.; Costa, M.; Coe, M.T.; DeFries, R.; Gibbs, H.K.; Howard, E.A.; Olson, S.; Patz, J.; Ramankutty, N.; et al. Amazonia revealed: Forest degradation and loss of ecosystem goods and services in the Amazon Basin. *Front. Ecol. Environ.* **2007**, *5*, 25–32. [[CrossRef](#)]
29. Herzog, S.K.; Martínez, R.; Jørgensen, P.M.; Tiessen, H. (Eds.) *Climate Change and Biodiversity in the Tropical Andes*; IAI: Montevideo, Uruguay, 2017.
30. Rimal, B.; Sharma, R.; Kunwar, R.; Keshtkar, H.; Stork, N.E.; Rijal, S.; Rahman, S.A.; Baral, H. Effects of land use and land cover change on ecosystem services in the Koshi River Basin, Eastern Nepal. *Ecosyst. Serv.* **2019**, *38*, 100963. [[CrossRef](#)]
31. Mondal, A.; Kundu, S.; Chandniha, D.K.; Shukla, R.; Chandniha, S.; Mishra, P.K. Comparison of support vector machine and maximum likelihood classification technique using satellite imagery. *Int. J. Remote Sens. GIS* **2012**, *1*, 116–123.

32. Zelený, J.; Mercado-Bettín, D.; Müller, F. Towards the evaluation of regional ecosystem integrity using NDVI, brightness temperature and surface heterogeneity. *Sci. Total Environ.* **2021**, *796*, 148994. [CrossRef]
33. Valentini, E.; Taramelli, A.; Filippini, F.; Giulio, S. An effective procedure for EUNIS and Natura 2000 habitat type mapping in estuarine ecosystems integrating ecological knowledge and remote sensing analysis. *Ocean Coast. Manag.* **2015**, *108*, 52–64. [CrossRef]
34. Madhu, K.; Pauliuk, S.; Dhathri, S.; Creutzig, F. Understanding environmental trade-offs and resource demand of direct air capture technologies through comparative life-cycle assessment. *Nat. Energy* **2021**, *6*, 1035–1044. [CrossRef]
35. ECOLAP and MAE. Ubicación Geográfica de la Región Sierra Escala 1: 2'700.000 aprox. Available online: <https://www.parks-and-tribes.com/national-parks/parque-nacional-llanganates/parque-nacional-llanganates.pdf> (accessed on 3 January 2023).
36. Ron, S.R.; Navarrete, M.J.; Venegas, P. Two new species of frogs of the genus *Pristimantis* from Llanganates National Park in Ecuador with comments on the regional diversity of Ecuadorian *Pristimantis* (Anura, Craugastoridae). *Zookeys* **2016**, *593*, 139–162. [CrossRef]
37. Ortega, J.A.; Brito, J.; Ron, S.R. Six new species of *Pristimantis* (Anura: Strabomantidae) from Llanganates National Park and Sangay National Park in Amazonian cloud forests of Ecuador. *PeerJ* **2022**, *10*, e13761. [CrossRef]
38. Orozco, C.I.; Pérez, Á.J.; Romelroux, K.; Aldana, J.M. The discovery of a new species of *Brunellia* (Brunelliaceae) with ephemeral petals from Llanganates National Park, Ecuador. *Phytotaxa* **2017**, *311*, 263–269. [CrossRef]
39. Guevara, M.-F.; Salazar, P.; Mátyás, B.; Ordoñez, M.-E. Xylariales: First results of mycological exploration in the Sangay and Llanganates National Park, Ecuador. *F1000Research* **2018**, *7*, 222. [CrossRef]
40. Palacios, J.; Naveda-Rodríguez, A.; Zapata-Ríos, G. Large mammal richness in Llanganates National Park, Ecuador. *Mammalia* **2017**, *82*, 309–314. [CrossRef]
41. Villota, A.; León-Yáñez, S.; Behling, H. Mid- and late Holocene vegetation and environmental dynamics in the Llanganates National Park, Anteojos Valley, central Ecuadorian Andes. *Palynology* **2014**, *39*, 350–361. [CrossRef]
42. Gong, J.; Sui, H.; Ma, G.; Zhou, Q. A Review of Multi-Temporal Remote Sensing Data Change Detection Algorithms. 2008. Available online: <https://www.researchgate.net/publication/241682221> (accessed on 3 January 2023).
43. Cooley, T.; Anderson, G.P.; Felde, G.W.; Hoke, M.L.; Ratkowski, A.J.; Chetwynd, J.H.; Gardner, J.A.; Adler-Golden, S.M.; Matthew, M.W.; Berk, A.; et al. FLAASH, a MODTRAN4-based Atmospheric Correction Algorithm, Its Application and Validation. In Proceedings of the IEEE International Geoscience and Remote Sensing Symposium, Toronto, ON, Canada, 24–28 June 2002.
44. Uzoukwu, C.U. Using GIS to Detect Changes in Land Use Land Cover for Electrical Transmission Line Siting and Expansion Planning in Winona County. 2010. Available online: <http://www.gis.smu.edu> (accessed on 3 January 2023).
45. Gomez-Chova, L.; Tuia, D.; Moser, G.; Camps-Valls, G. Multimodal Classification of Remote Sensing Images: A Review and Future Directions. *Proc. IEEE* **2015**, *103*, 1560–1584. [CrossRef]
46. Foody, G.M.; Mathur, A. Toward intelligent training of supervised image classifications: Directing training data acquisition for SVM classification. *Remote Sens. Environ.* **2004**, *93*, 107–117. [CrossRef]
47. Polat, N.; Kaya, Y. Intercontinental Geoinformation Days an Investigation of Supervised LCLU Classification Performance over UAV Based Orthophoto. Available online: <http://igd.mersin.edu.tr/2020/> (accessed on 3 January 2023).
48. Ehsan, S.; Kazem, D. Analysis of land use-land covers changes using normalized difference vegetation index (NDVI) differencing and classification methods. *Afr. J. Agric. Res.* **2013**, *8*, 4614–4622. [CrossRef]
49. Sathya, P. Analysis of Supervised Image Classification Method for Satellite Images. *Int. J. Comput. Sci. Res. (IJCSR)* **2017**, *5*, 16–19.
50. Zaidi, S.M.; Akbari, A.; Abu Samah, A.; Kong, N.S.; Gisen, J.I.A. Landsat-5 Time Series Analysis for Land Use/Land Cover Change Detection Using NDVI and Semi-Supervised Classification Techniques. *Pol. J. Environ. Stud.* **2017**, *26*, 2833–2840. [CrossRef]
51. Conese, C.; Maselli, F. Use of Error Matrices to Improve Area Estimates with Maximum Likelihood Classification Procedures. *Remote Sens. Environ.* **1992**, *40*, 113–124. [CrossRef]
52. Niu, X.; Hu, Y.; Lei, Z.; Wang, H.; Zhang, Y.; Yan, H. Spatial and Temporal Evolution Characteristics of Land Use/Cover and Its Driving Factor in Cambodia during 2000–2020. *Land* **2022**, *11*, 1556. [CrossRef]
53. Awuah, K.T.; Nölke, N.; Freudenberg, M.; Diwakara, B.; Tewari, V.; Kleinn, C. Spatial resolution and landscape structure along an urban-rural gradient: Do they relate to remote sensing classification accuracy?—A case study in the megacity of Bengaluru, India. *Remote Sens. Appl. Soc. Environ.* **2018**, *12*, 89–98. [CrossRef]
54. Elkie, P.; Rempel, R.; Angus, P. Patch Analyst User's Manual. 1999. Available online: <https://www.yumpu.com/en/document/read/29088001/patch-analyst-users-manual> (accessed on 3 January 2023).
55. Sapena, M.; Ruiz, L. Guía de Usuario IndiFrag v2.1. 2016. Available online: https://cgat.webs.upv.es/BigFiles/indifrag/GuiaUsuario_IndiFrag_v2.1.pdf (accessed on 3 January 2023).
56. Toulkeridis, T.; Tamayo, E.; Simón-Baile, D.; Merizalde-Mora, M.J.; Reyes-Yunga, D.F.R.; Viera-Torres, M.; Heredia, M. Climate Change according to Ecuadorian academics—Perceptions versus facts. *Granja* **2020**, *31*, 21–49. [CrossRef]
57. Vaca, A.; Arroyo, C.R.; Debut, A.; Toulkeridis, T.; Cumbal, L.; Mato, F.; Aguilera, M.C.D.A.E. Characterization of Fine-grained Material Ejected by the Cotopaxi Volcano Employing X-ray Diffraction and Electron Diffraction Scattering Techniques. *Biol. Med.* **2016**, *8*. [CrossRef]
58. Biratu, A.A.; Bedadi, B.; Gebrehiwot, S.G.; Melesse, A.M.; Nebi, T.H.; Abera, W.; Tamene, L.; Egeru, A. Impact of Landscape Management Scenarios on Ecosystem Service Values in Central Ethiopia. *Land* **2022**, *11*, 1266. [CrossRef]

59. Wang, Y.; Rao, Y.; Zhu, H. Revealing the Impact of Protected Areas on Land Cover Volatility in China. *Land* **2022**, *11*, 1361. [[CrossRef](#)]
60. Zhao, S.; Fan, Z.; Gao, X. Spatiotemporal Dynamics of Land Cover and Their Driving Forces in the Yellow River Basin since 1990. *Land* **2022**, *11*, 1563. [[CrossRef](#)]
61. Lozano, P.; Cabrera, O.; Peyre, G.; Cleef, A.; Toulkeridis, T. Plant Diversity and Composition Changes along an Altitudinal Gradient in the Isolated Volcano Sumaco in the Ecuadorian Amazon. *Diversity* **2020**, *12*, 229. [[CrossRef](#)]
62. Arroyo-Rodríguez, V.; Arasa-Gisbert, R.; Arce-Peña, N.P.; Cervantes-López, M. Determinantes de la Biodiversidad en Paisajes Antrópicos: Una Revisión Teórica. Universidad Autónoma del Estado de Hidalgo y Libermex. 2019. Available online: https://www.researchgate.net/publication/338557779_Determinantes_de_la_biodiversidad_en_paisajes_antropicos_Una_revision_teorica (accessed on 3 January 2023).
63. Pal, S.; Singha, P.; Lepcha, K.; Debanshi, S.; Talukdar, S.; Saha, T.K. Proposing multicriteria decision based valuation of ecosystem services for fragmented landscape in mountainous environment. *Remote Sens. Appl. Soc. Environ.* **2020**, *21*, 100454. [[CrossRef](#)]
64. Popov, M.; Michaelides, S.; Stankevich, S.; Kozlova, A.; Piestova, I.; Lubskiy, M.; Titarenko, O.; Svideniuk, M.; Andreiev, A.; Ivanov, S. Assessing long-term land cover changes in watershed by spatiotemporal fusion of classifications based on probability propagation: The case of Dniester river basin. *Remote Sens. Appl. Soc. Environ.* **2021**, *22*, 100477. [[CrossRef](#)]
65. Sugianto, S.; Deli, A.; Miswar, E.; Rusdi, M.; Irham, M. The Effect of Land Use and Land Cover Changes on Flood Occurrence in Teunom Watershed, Aceh Jaya. *Land* **2022**, *11*, 1271. [[CrossRef](#)]
66. Xu, C.; Fu, H.; Yang, J.; Wang, L. Assessment of the Relationship between Land Use and Flood Risk Based on a Coupled Hydrological–Hydraulic Model: A Case Study of Zhaojue River Basin in Southwestern China. *Land* **2022**, *11*, 1182. [[CrossRef](#)]
67. López-Rodríguez, F.; Rosado, D. Management effectiveness evaluation in protected areas of southern Ecuador. *J. Environ. Manag.* **2017**, *190*, 45–52. [[CrossRef](#)]
68. Yi, H.; Güneralp, B.; Filippi, A.M.; Kreuter, U.P.; Güneralp, İ. Impacts of Land Change on Ecosystem Services in the San Antonio River Basin, Texas, from 1984 to 2010. *Ecol. Econ.* **2017**, *135*, 125–135. [[CrossRef](#)]
69. Strange, E.M.; Fausch, K.D.; Covich, A.P. Sustaining Ecosystem Services in Human-Dominated Watersheds: Biohydrology and Ecosystem Processes in the South Platte River Basin. *Environ. Manag.* **1999**, *24*, 39–54. [[CrossRef](#)]
70. Terrado, M.; Momb Blanch, A.; Bardina, M.; Boithias, L.; Munné, A.; Sabater, S.; Solera, A.; Acuña, V. Integrating ecosystem services in river basin management plans. *J. Appl. Ecol.* **2016**, *53*, 865–875. [[CrossRef](#)]
71. Sobhani, P.; Esmailzadeh, H.; Mostafavi, H. Simulation and impact assessment of future land use and land cover changes in two protected areas in Tehran, Iran. *Sustain. Cities Soc.* **2021**, *75*, 103296. [[CrossRef](#)]
72. Zefrehei, A.R.P.; Hedayati, S.; Sahraei, H. Long-term dynamic analysis based on Landsat imagery in the Gorgan Bay-Gomishan Wetland, Iran. *Casp. J. Environ. Sci.* **2022**, *20*, 721–727. [[CrossRef](#)]

Disclaimer/Publisher’s Note: The statements, opinions and data contained in all publications are solely those of the individual author(s) and contributor(s) and not of MDPI and/or the editor(s). MDPI and/or the editor(s) disclaim responsibility for any injury to people or property resulting from any ideas, methods, instructions or products referred to in the content.